DMD Fast Forward. Published on April 29, 2016 as DOI: 10.1124/dmd.116.069377
This article has not been copyedited and formatted. The final version may differ from this version.

Title Page

Biotransformation capacity of carboxylesterase in skin and keratinocytes for the penta-ethyl ester prodrug of DTPA

Jing Fu, Matthew Sadgrove, Lesley Marson, Michael Jay

Center for Nanotechnology in Drug Delivery, Division of Molecular Pharmaceutics, University of North Carolina Eshelman School of Pharmacy, Chapel Hill, North Carolina (J.F., M.S., L.M., M.J.)

DMD Fast Forward. Published on April 29, 2016 as DOI: 10.1124/dmd.116.069377
This article has not been copyedited and formatted. The final version may differ from this version.

Running Title Page

a) Prodrug hydrolysis by CES in epidermal keratinocytes

b) Corresponding author's name: Michael Jay, Ph.D.

Address:

Marsico Hall Room 4012

125 Mason Farm Rd, Chapel Hill, NC, 27599

UNC Eshelman School of Pharmacy

University of North Carolina at Chapel Hill

Telephone: 919.962.0082

Fax: 919.966.0197

Email address: mjay@email.unc.edu

c) The number of text pages: 31

The number of tables: 2

The number of figures: 6

The number of references: 37

Words in abstract: 250

Words in introduction: 630

Words in discussion: 1258

DMD Fast Forward. Published on April 29, 2016 as DOI: 10.1124/dmd.116.069377
This article has not been copyedited and formatted. The final version may differ from this version.

d) List of nonstandard abbreviations

ACN: Acetonitrile

BNPP: Bis-para-nitrophenylphosphate

CES1: Human carboxylesterase 1

CES2: Human carboxylesterase 2

C2E4: DTPA tetra-ethyl ester; metabolite of C2E5

C2E5: Penta-ethyl ester prodrug of the chelating agent DTPA

DTPA: Diethylene triamine pentaacetic acid

GAPDH: Glyceraldehyde-3-phosphate dehydrogenase

HEKa: Adult human epithelial kerotinocytes

HEKn: Neonatal human epithelial kerotinocytes

Hu Skin: Human skin

4NP: 4-Nitrophenol

4NPV: 4-Nitrophenyl valerate

*p*NPA: 4-Nitrophenyl acetate

RT-qPCR: Real-time polymerase chain reaction

S9: Supernatant after centrifugation at 9000*g*

Abstract

The penta-ethyl ester prodrug of the chelating agent diethylene triamine pentaacetic acid (DTPA), referred to as C2E5, effectively accelerated clearance of americium after transdermal delivery. Carboxylesterases (CESs) play important roles in facilitating C2E5 hydrolysis. However, whether CESs in human skin hydrolyze C2E5 remains unknown. We evaluated the gene and protein expression of CESs in distinctive human epidermal cell lines: HEKa, HEKn, HaCaT and A431. The substrates, *p*-nitrophenyl acetate (*p*NPA) and 4-nitrophenyl valerate (4-NPV), were used to access esterase and CES activity. C2E5 hydrolysis was measured by radiometric HPLC after incubating [^{14}C]-C2E5 with S9 fractions prepared from skin cell lines with analysis. CESs specific inhibitors were used to access metabolism in human skin S9 fractions with analysis by LC/MS/MS. We identified the CES1 and CES2 bands in the western blot. The gene expression of these enzymes was supported by a real-time polymerase chain reaction (RT-qPCR). *p*NPA and 4-NPV assays demonstrated esterases and CESs activity in all the cell lines that were comparable to human skin S9 fractions. The prodrug C2E5 was hydrolyzed by skin S9 fractions resulting in a primary metabolite, C2E4. In human skin S9 fractions, inhibition of C2E5 hydrolysis was greatest with a pan CES inhibitor (benzil). CES1 inhibition (troglitazone) was greater than CES2 (loperamide), suggesting a primary metabolic role for CES1. These results indicate that human keratinocyte cell lines are useful for the evaluation of human cutaneous metabolism and absorption of ester-based prodrugs. However, keratinocytes from skin provide a small contribution to the overall metabolism of C2E5.

DMD Fast Forward. Published on April 29, 2016 as DOI: 10.1124/dmd.116.069377
This article has not been copyedited and formatted. The final version may differ from this version.

Introduction

Transdermal drug delivery is non-invasive, can be self-administered, avoids first-pass metabolism, and is well-suited to pediatric populations and particular patient groups who have trouble swallowing (Zempsky, 1998). In addition, transdermal products are attractive due to their sustained zero-order systemic release profile (Naik et al., 2000). However, to reach the systemic circulation, drug molecules need to pass through the skin's multiple barriers including the hydrophobic environment of the stratum corneum, the epidermis and the dermis to reach the vascularized hypodermis. These barriers effectively limit direct transdermal drug delivery to molecules that possess aqueous solubility in physiological pH (> 1 mg/ml, pH 5-9), a low molecular weight (usually <500 Daltons), moderate lipophilicity (oil-water partition coefficient $K_{o/w}$ 10 – 1000), and those that require a moderate daily dosage (< 10 mg/day) (Naik et al., 2000, Perumal et al., 2013). A growing number of drugs, that have many of the properties listed above, have been approved for transdermal delivery. These include estradiol, fentanyl, lidocaine and testosterone patches and ultrasonic delivery systems for analgesia (Nitti, 2003, Prausnitz and Langer, 2008).

In addition to the physical barriers, cutaneous metabolism via local phase I and phase II metabolic enzymes can also reduce bioavailability (Esser and Gotz, 2013, Zhang et al., 2009). Cytochrome P450 enzymes are clearly expressed in organotypic skin models (Saeki et al., 2002, Swanson, 2004). In human skin, CYP families 1, 2 and 3 are responsible for the metabolism of the majority of drugs and other xenobiotics (Du et al., 2004). Xenobiotic metabolizing enzymes are located in the epidermis and dermis where hair follicles, sebaceous and sweat glands are located (Scheuplein and Blank, 1971; Sugibayashi et al., 1999). The study of dermal metabolism is complicated by significant interspecies differences in xenobiotic metabolism (Inoue et al.,

1980; Prusakiewicz et al., 2006; Fu et al., 2015). Therefore, ideally, metabolism should be investigated in human skin tissues.

Enzymatic metabolism in the skin can be utilized to bio-activate prodrug molecules and to improve dermal or transdermal delivery. For example, morphine propionate and morphine enanthate are two alkyl ester prodrugs of morphine that have been shown to enhance dermal delivery of morphine by 2- and 5-fold, respectively (Wang et al., 2007). Many prodrugs, including these two morphine prodrugs, are formed by esterification of the active molecule. The added ester moiety can be used to alter the physicochemical properties of the molecule and improve transdermal absorption (Wang et al., 2007). Once absorbed into the skin, enzymatic hydrolysis of the prodrug by esterases releases the active drug.

Carboxylesterases (CES1 and CES2) are involved in the metabolism of xenobiotics. For example, CES1 activates prodrugs of angiotensin-converting enzyme inhibitors and CES2 activates the anticancer prodrug CPT-11 (Bencharit et al., 2002, Thomsen et al., 2014). In humans, CES1 and CES2 expression is ubiquitous; however, CES1 predominates in most organs (Satoh et al., 2002). Although CESs are known to be expressed in human skin, information on their role in the metabolism of topically applied drugs and prodrugs is limited (Zhu et al., 2007).

We have developed a penta-ethyl ester prodrug of the chelating agent diethylene triamine pentaacetic acid (DTPA), referred to as C2E5 (Figure 1), to enhance clearance (decorporation) of transuranic radionuclides (Zhang et al., 2013b). C2E5 is metabolized by CESs (Fu et al., 2015) and the physiochemical properties of C2E5 (CLogP of 4.7, with a molecular weight of 533 Daltons) suggest that it would be a good candidate for transdermal delivery. Evidence supporting transdermal application of C2E5 was reported in rat *in vivo* transdermal pharmacokinetics and efficacy studies (Zhang et al., 2013b). Therefore, the first objective of the current work was to

DMD Fast Forward. Published on April 29, 2016 as DOI: 10.1124/dmd.116.069377
This article has not been copyedited and formatted. The final version may differ from this version.

assess the expression of CES isoforms in four different human skin cell lines. The second objective was to determine the capacity of the CESs in each cell line to metabolize the prodrug C2E5.

DMD Fast Forward. Published on April 29, 2016 as DOI: 10.1124/dmd.116.069377
This article has not been copyedited and formatted. The final version may differ from this version.

Materials and Methods

Materials. [^{14}C]-DTPA penta-ethyl ester ([^{14}C]-C2E5; 55 mCi/mmol, 1mCi/ml) was purchased from American Radiolabeled Chemicals, Inc. (St. Louis, MO). Ultima-Flo AP scintillation fluid was obtained from PerkinElmer Life and Analytical Sciences (Waltham, MA). Acetonitrile (ACN), 4-nitrophenyl valerate (4-NPV), *p*-nitrophenyl acetate (*p*NPA), Dulbecco's modified Eagle's medium, 0.25% trypsin-EDTA, and Dulbecco's phosphate buffered saline (PBS) were purchased from Sigma Aldrich (St. Louis, MO). Penicillin-streptomycin was purchased from Invitrogen Corporation (Carlsbad, CA). Fetal bovine serum was purchased from Cansera International Inc. (Rexdale, ON, Canada). Human female skin S9 fractions were purchased from BioreclamationIVT (Hicksville, NY).

Cell Culture. HaCaT cells, immortal human keratinocytes, and A431, an immortalized epidermoid carcinoma derived, were kindly provided by Dr. Zhi Liu (Lineberger Comprehensive Cancer Center, Chapel Hill, NC). Primary neonatal human epithelial kerotinocytes (HEKn) and adult human epithelial kerotinocytes (HEKa) cells were obtained commercially (Gibco by Life Technologies, Grand Island, NY). HaCaT and A431 were maintained in 10% fetal bovine serum and Dulbecco's modified eagle medium/high glucose medium (Gibco) containing 10% fetal calf serum, penicillin (10,000 units/ml) and streptomycin (10 mg/ml) until sub-confluence was reached (after 48 h). HEKn and HEKa were cultured in EpiLife medium (Gibco), supplemented with 1% EpiLife® defined growth supplement and 0.1% calcium chloride ($CaC1_2$) (Gibco). All incubations were conducted at 37±1°C, 95% air/5% CO_2, and saturated humidity.

DMD Fast Forward. Published on April 29, 2016 as DOI: 10.1124/dmd.116.069377
This article has not been copyedited and formatted. The final version may differ from this version.

Preparation of Cell Supernatant (S9 fractions). For all cell lines, cytosolic S9 fractions were prepared as cited in literature (Imai et al., 2013). Protein concentrations were determined by the Pierce™ BCA protein assay (Thermo Fisher Scientific, Waltham, MA). Human liver S9 fractions (XenoTech, Kansas City, KS), human recombinant protein (BD Biosciences, Franklin Lakes, New Jersey), and human skin S9 fractions (BioreclamationIVT, Hicksville, NY) were purchased commercially.

Determination of the Gene Expression by Real-Time Polymerase Chain Reaction (RT-qPCR). HEKa, HEKn, HaCaT and A431 cells were seeded and grown in 15 ml in T75 tissue culture flasks. Expressions of the CESs genes were evaluated by RT-qPCR. Total RNA was extracted using the RNeasy Mini Kit (Qiagen, Cat. No.74134, Hilden, Germany) according to the manufacturer's instructions. Briefly, cell samples were lysed and homogenized using 1ml/10cm^2 cells of TRIzol (Ambion® by Life Technology) and then were isolated by QIAshredder columns (Qiagen Cat. No.79656) in a highly denaturing guanidine-thiocyanate containing buffer. Ethanol (70%) was added and the samples were applied to an RNeasy Mini Spin Column (Qiagen). RNA was bound to the membrane of the column and contaminants were washed away. Subsequently, RNA was eluted from the column using 30 µl of water. The concentration and purity of the total RNA was determined using the Nanodrop 2000 method (Thermo Scientific,Wilmington, DE). cDNAs were prepared by reverse transcription of total RNA using the iScript™ cDNA synthesis kit (Bio-Rad cat #170-8891, Hercules, CA) and stored at -20ºC until qPCR amplification. qPCR reactions were prepared using the 2X iTaq™ Universal Probes Supermix, TaqMan® CES1, CES2 and glyceraldehyde-3-phosphate dehydrogenase (GAPDH) primers, (TaqMan® Gene Expression Assays Rack ID: 14429192. Primers: Hs00275607_m1 for CES1, Hs01077945_m1 for CES2 and Hs02758991_g1 for GAPDH) (Applied Biosystems, Foster City, CA) and

DMD Fast Forward. Published on April 29, 2016 as DOI: 10.1124/dmd.116.069377
This article has not been copyedited and formatted. The final version may differ from this version.

nuclease-free water (Qiagen) cDNA was diluted 5- fold and qPCR was performed by the TaqMan® Gene Expression Assay (Bio-Rad). The PCR amplification was conducted in a total volume of 20 µl containing universal PCR master mixture (10 µl), gene-specific TaqMan® assay mixture (1 µl), diluted cDNA (5 µl) and nuclease-free water (4 µl). The cycling profile was 50°C for 2 min, 95°C for 10 min, followed by 40 cycles of 15 s at 95°C and 1 min at 60°C, as recommended by the manufacturer. Amplification and quantification were done with the Applied Biosystems 7900HT Real-Time PCR System (Foster City, CA). All samples were analyzed in triplicate and the signals were normalized to GAPDH and then expressed as relative levels of mRNA. The CES1 probe recognized both CES1A1 and CES1A2; these enzymes are identical although distinct genes encoded. GAPDH was included in the study as the loading control.

Quantification of Gene Expression. Relative RNA expression levels were determined from delta Ct values using the expression of the GAPDH gene as an internal control. The RT-qPCR assay was performed in triplicate for each sample. For each replicate, the CES Ct was normalized to the GAPDH Ct [$\Delta Ct = Ct_{[Target]}-Ct_{[Gapdh]}$] before the mean and SEM ΔCt were calculated.

Determination of the Protein Expression. Western blot studies were conducted to explore CES1 and CES2 expression in the different human skin cell lines. CES1 and CES2 antibodies were purchased from Abcam (Cambridge, England). Protein concentrations were determined using the Pierce™ BCA Protein Assay (Thermo Fisher Scientific). Total protein lysate (30 µg) was run on a NuPAGE™ 4–12% Bis-Tris Gel (Bio-Rad) at 120 V for 1 h. Following electrophoresis, the proteins were transferred by blotting onto 0.45 µm polyvinyl difluoride membranes (Thermo Fisher Scientific) at 350 mA for 1.25 h in transfer buffer (Bio-Rad). The

membrane was blocked in 5% skimmed milk powder in Tris-buffered saline/0.05% Tween for 1 h before overnight incubation with primary antibody: monoclonal hCES1 or hCES2 (Sigma-Aldrich) at 1:1000 dilution or GAPDH (Abcam) at 1:10000 dilution. The membranes were washed and incubated with a secondary antibody, horseradish peroxidase-conjugated goat anti-rabbit (Sigma-Aldrich) at 1:10000 dilution for 1 h. Finally, the membranes were incubated briefly in SuperSignal® Stable Peroxide Solution together with SuperSignal® West Pico Luminol/Enhancer Solution (Thermo Fisher Scientific) and immediately imaged. The chemiluminescent signal was registered with a FluorChem 8000 camera (Alpha Innotech Corp, San. Leandro, CA). Human liver and intestine S9 fractions served as positive controls for CES1 and CES2, respectively.

Determination of Enzyme Activity by *p*NPA Assay and 4-NPVAssay. Total esterase and CES-specific enzyme activity was measured using established substrates *p*NPA (100 μM) and 4-NPV (100 μM), respectively (Testa B and Mayer MJ, 2006). Hydrolysis of the freshly prepared substrates was carried out in 96 well plates with a total volume of 100 μl/well. Reactions were initiated by mixing 1 μl of substrate with diluted S9 samples (0.1 mg/ml). The rates of hydrolysis of *p*NPA and 4-NPV were determined spectrophotometrically by measuring reaction products at 402 nm after 10 min incubation at 37°C as previously described (Williams, 2008) using a UV spectrometer (BioTek, Winooski, VT).

Determination of C2E5 Hydrolysis by High Performance Liquid Chromatography-Radiomatic Flow Scintillation Analyzers (HPLC-FSA). [^{14}C]-C2E5 (1 μM, 0.55 nCi) was pre-incubated in 0.1 M phosphate buffer (pH 7.4) for 5 min at 37°C. Reactions were initiated by the addition of S9 fractions (1 mg/ml) from different cell lines (HEKa, HEKn, HaCaT and A431)

in a total volume of 100 µl; boiled S9 fractions were used as a blank to correct for non-enzymatic C2E5 degradation. The reactions were terminated by adding an equal volume of ice-cold acetonitrile (ACN), followed by centrifugation at 14,000*g* for 15 min at 4°C. The supernatant was transferred to HPLC vials for analysis as previously described (Fu et al., 2015). Representative radio-chromatograms illustrate a C2E5 peak generated from the boiled S9 fractions and C2E5 and the presences of a metabolite, C2E4, in human skin S9 fractions (Supplemental Figures 1 and 2).

Sample Preparation for Human Skin S9 fraction-Mediated C2E5 Hydrolysis with and without Inhibitors. Experiments were designed to examine the effect of specific inhibitors on C2E5 hydrolysis in human skin S9 fractions. The following inhibitors were selected: benzil (10 µM) was chosen as a pan CES inhibitor (Wadkins et al., 2005), troglitazone (10 µM) as a CES1 specific inhibitor (Fukami et al., 2010), loperamide (100 µM) as a CES2 specific inhibitor (Williams et al., 2011) and BNPP (1 mM) as a non-specific esterase inhibitor (Li et al., 2007). Inhibitors were incubated with human skin S9 fractions for 30 min at 37°C before the reaction was initiated. All reactions were initiated by the addition of S9 fractions (0.5 and 1 mg/ml) to prepared C2E5 in water to result a final C2E5 concentration of 0.5 µM at 37°C. Reactions were terminated after 120 min by adding an equal volume of ice-cold acetonitrile with 2% of formic acid, followed by centrifugation at 14,000 *g* for 15 min at 4°C. Liver S9 fractions (1 mg/ml) were used as a positive control and boiled S9 fractions were used as negative controls. Reactions were performed in triplicate. The standards used to generate the LC/MS/MS C2E5 calibration curve were prepared by spiking boiled S9 fractions with C2E5 and processed as described above.

LC/MS/MS Chromatographic and Spectroscopic Conditions. Chromatographic separation from matrix components was achieved using reverse-phase chromatography on an YMC ODS-

AM C18 (100 x 2 mm, 3 µm) column. Gradient elution was used based on a combination of water with 0.1% formic acid (A) and acetonitrile with 0.1% formic acid (B). The mobile phase was initiated at 13% B increasing to 40% B by 1 min, to 60% B by 6 min and to 95% B by 6.2 min. The mobile phase was held at 5% A and 95% B from 6.2 min to 6.5 min when a post-run cycle that included isopropyl alcohol (C) was initiated. Between 6.5 min and 7 min solvent B (95%) was gradually replaced with solvent C (95%). The mobile phase was then held at 5% A 95% C until 7.5 min before gradually returning to initial conditions (87% A, 13% B, 0% C) after 8.5 min, which were maintained for 1.5 min prior to the next injection. The flow rate was 300 µl/min and the injection volume was 5 µl. The column oven temperature was set to 40°C. C2E5 was detected on a triplequadrupole mass spectrometer (Thermo TSQ Quantum Access) using electrospray ionization (ESI) in the positive-ion mode. The ionization source and collision parameters were optimized to give maximum analyte signal intensity (Spray Voltage 3500V; Sheath and Auxiliary gas nitrogen, 10 and 25 psi, respectively; Collision gas Argon @ 1.5 mTorr; Collision energy 35 eV). The mass spectrometer was set to carry out single reaction monitoring (SRM) for the precursor → product ion transitions m/z 534 → 216 (C2E5) and m/z 506 → 188 (C2E4) at a retention times of 3.6 and 2.8 min, respectively. For C2E5 quantification, a calibration plot of analyte peak area against nominal C2E5 concentration (20 – 1000 ng/ml) was constructed from a quadratic equation with a 1/concentration^2 weighting. Representative chromatograms showed formation of C2E5 metabolite, C2E4. Representative chromatograms illustrate a C2E5 peak generated from the boiled S9 fractions and C2E5 and the presences of a metabolite, C2E4, in human skin S9 fractions (Supplemental Figures 3 and 4).

Data analysis. The data were processed by Graph Pad Prism 5.0, and are presented as mean ± SEM.

DMD Fast Forward. Published on April 29, 2016 as DOI: 10.1124/dmd.116.069377
This article has not been copyedited and formatted. The final version may differ from this version.

Results

Gene Expression of Carboxylesterase in HEKa, HEKn HaCaT, A431 cells, and Human Skin Tissue. The mRNA expression of CES1 was primarily detected in human skin tissue. A small amount was detected in HEKa and HEKn cells, and none was detected in HaCaT and A431 cells (Figure 2A). In contrast, mRNA expression of CES2 was detected in all cells. Human skin CES2 expression was about 2-fold higher than HEKa, HEKn and HaCaT and 10-fold higher than A431 expression (Figure 2B). CES1 expression in the human skin was about 25-fold greater than CES2 expression. However, the human skin total RNA was obtained from only one human subject and inter-individual variability could affect these comparative results.

Protein Expression of Carboxylesterase in HEKa, HEKn, HaCaT, A431 cells and Human Skin Tissue. Human liver and intestine S9 fractions were used as positive controls. CES1 protein expression was detected in human skin S9 fractions. The band for CES1 in human skin (30 μg of skin sample) was considerably lighter than the CES1 band in human liver S9 fractions (5 μg of liver sample). There was little evidence of CES1 in HEKn, HaCaT and A431 cells (Figure 3A). Meanwhile, CES2 protein expression was detected in HEKn, HaCaT, human skin and human intestine S9 fractions (Figure 3B). The bands indicated that more CES2 was present in HEKn compared to HaCaT. Little evidence for CES2 in A431 was observed (Figure 3B).

Hydrolysis Activity of *p*NPA and 4-NPV in HEKa, HEKn, HaCaT, A431 cells and Human Skin Tissue. Enzymatic activity was determined using *p*NPA (esterases) and 4-NPV (CESs) assays with human liver S9 fractions as a control. The *p*NPA assay demonstrated that the S9 fractions from human skin cell lines exhibited esterase activity (Figure 4A). *p*NPA hydrolysis activity in the cultured cells was slightly lower than in human skin S9 fractions and 5- to 10-fold

lower than in human liver S9 fractions (Table 1). For example, HEKn displayed approximately 20% of the esterase activity of the liver. When the amount of protein was standardized across all the samples, the catalytic rate of esterase in HEKn was the highest among all cell lines. The 4-NPV assay showed that CES activity was present in all of the tested cells; the catalytic rate of CES in HEKn cell lines was the greatest (Figure 4B). 4-NPV hydrolytic activity in the cultured cells was comparable to or slightly lower than in human skin S9 fractions and 2- to 5-fold lower than in human liver S9 fractions (Table 2). For example, HEKn displayed approximately 60% of the CES activity of the liver.

Hydrolytic Activity of Penta-ethyl Ester Prodrug of DTPA (C2E5) in HEKa, HEKn, HaCaT and A431 Cell Lines. S9 fractions produced from HEKa, HEKn, HaCaT hydrolyzed [^{14}C]-C2E5 (1μM) to the primary metabolite, C2E4. Little hydrolysis was observed in the S9 fractions of A431 cells (Figure 5). The hydrolytic rates of C2E5 by HEKa, HEKn, HaCaT and A431 cells were 7.12, 2.63, 3.80 and 0.66 pmol/mg/min, respectively.

Inhibition of Hydrolytic Activity of Penta-ethyl Ester Prodrug of DTPA (C2E5) in Human Skin S9 Fractions. Near complete (98.6%) hydrolysis was seen in human liver S9 fractions, while human skin S9 fractions showed 62.8% loss of the parent drug (C2E5, Figure 6). As expected, addition of the non-specific esterase inhibitor, BNPP, totally blocked the hydrolysis of C2E5. Addition of the inhibitors benzil (pan CESs) troglitazone (CES1) and loperamide (CES2) resulted in 10.6%, 40.68%, and 77.68% loss of parent drug C2E5, respectively. These data suggest that both CES1 and CES2 hydrolyze C2E5, but the hydrolysis is primarily via CES1.

Discussion

As transdermal delivery technology becomes more common, questions remain as to how and whether ester-based prodrugs pass through the skin and whether hydrolysis during this transition affects the absorption, distribution, metabolism and excretion (ADME) of the drug. Because of the interspecies differences in hydrolysis profiles, skin derived from animals may be very different from human skin (Tauber, U. R and Rost KL, 1987, Prusakiewicz et al., 2006, Hewitt et al., 2001). Therefore, alternative methods to examine human specific hydrolysis are needed during drug development. Previously, we reported that CESs play an important role in the metabolism of the ester-based prodrug, C2E5, which is being investigated as a decorporation agent for contamination with transuranic elements (Zhang et al., 2013b). The present study characterized CES expression and activity in human skin tissue and different human keratinocyte cell lines and demonstrated the role of CES in facilitating C2E5 hydrolysis in skin during transdermal delivery. In addition, the prodrug, C2E5, was hydrolyzed in all skin cell lines examined and HEKa may be one of the most appropriate cell lines to study for transdermal delivery.

CES1 and CES2 proteins were expressed in human skin S9 fractions. RT-qPCR clearly showed the greater expression of CES1 mRNA compared to CES2 mRNA, which supports a previous report of greater CES1 expression in human skin microsomes (Jewell et al., 2007). As expected, measurement of total esterase activity using the *p*NPA assay (Imai et al., 2013) revealed much less activity in the skin compared to the liver (Figure 4A). However, the 4-NPV assay, which measures CES activity (Williams et al., 2011) showed that total CES activity was only 2-fold lower in the skin than in the liver (Figure 4B), confirming the potential for human skin to

DMD Fast Forward. Published on April 29, 2016 as DOI: 10.1124/dmd.116.069377
This article has not been copyedited and formatted. The final version may differ from this version.

contribute to the metabolism of ester compounds when applied transdermally (Wang et al., 2007).

As an alternative to human skin, we assessed different human keratinocyte cell culture models for their utility as surrogates in investigating transdermal drug metabolism. The keratinocyte tumor cell line A431 had no detectable CES1, and CES2 was expressed at barely detectable levels. Therefore, we concluded that A431 cell line is not a suitable model for investigating transdermal drug metabolism. Of the remaining keratinocyte cultures, our results demonstrated that while HEKa, HEKn and HaCaT express CES1, CES2 was more abundant across the various keratinocyte cell lines. These findings are consistent with the work of Zhu et al. who identified CES2 as the main CES in HaCaT cells (Zhu et al., 2007). Enzyme expression and activity in keratinocytes change over time in culture; cytochrome P450 enzymes are particularly vulnerable, but esterases and conjugated enzymes are also affected (Williams, 2008). This observation could explain our findings that CES2 expression was slightly lower in HaCaT cells compared to HEKa or HEKn cells, and that CES1 expression was greatly reduced or absent in all the cultured cells. HEKa and HEKn are primary cultures and, as such, may retain the greater enzymatic activity observed in human skin compared to the immortalized HaCaT cell line.

CES1 and CES2 are from the same family, known as 60-kDa serine esterases. While these two isoforms have a similar molecular weight, (CES1 is 62.5 kDa and CES2 is 60.0 kDa), they are structurally quite different. The isoelectric point of CES1 is 5.8 and CES2 is 4.9 and the sequence homology between the two enzymes is only 48% (Pindel et al., 1997). These structural differences result in different substrate specificity. CES1 tends to hydrolyze molecules with a small alcohol moiety more efficiently, while CES2 is more efficient at metabolizing molecules with a larger alcohol moiety and more lipophilic molecules (Brzezinski et al., 1994, Williams et

DMD Fast Forward. Published on April 29, 2016 as DOI: 10.1124/dmd.116.069377
This article has not been copyedited and formatted. The final version may differ from this version.

al., 2011). These differences in the substrate specificity of CES1 and CES2 could lead to differences in predicting skin absorption or metabolism. In different human cell lines and skin S9 fractions, we demonstrated CESs expression by western blot and RT-qPCR and confirmed enzyme activity with *p*NPA and 4-NPV assays; subsequently, we examined the metabolism of C2E5, a prodrug developed for transdermal delivery.

C2E5 is the penta-ethyl ester of DTPA, administered intravenously to treat plutonium, americium, and curium (Pu, Am and Cm) contamination. In vivo studies, in rats, report de-esterification of C2E5 mainly into the tri- and di-ethyl esters, C2E3 and C2E2, with some DTPA also present (Zhang et al., 2013b). In vitro binding experiments, using human, rat and dog plasma, suggest that C2E2 is an effective chelator of Am (Huckle et al., 2015a), and this hypothesis is supported by efficacy study following oral administration of C2E2 in beagle dogs (Huckle et al., 2015b). Thus, to be effective, when applied transdermally, C2E5 needs to be metabolized to C2E2 in the body. Sustained plasma concentrations of C2E2 are observed in rats following transdermal application of C2E5 in a non-aqueous gel (Zhang et al., 2013b) and this is associated with effective Am decorporation (Zhang et al., 2013a), suggesting that transdermal delivery of C2E5 to the active C2E2 is possible. In the present study, we used the S9 fractions model to assess the potential translation of these preclinical observations to human tissues.

Previously, we used a human recombinant protein system to examine human CES1 and CES2 mediated C2E5 hydrolysis; the results demonstrated that both CES1 and CES2 were reponsible for C2E5 hydrolysis. However, CES1 hydrolyzed C2E5 to a greater extent compared to CES2 (Fu et al., 2015). The results in the current study agree with our previous findings (Figure 5 and 6).

DMD Fast Forward. Published on April 29, 2016 as DOI: 10.1124/dmd.116.069377
This article has not been copyedited and formatted. The final version may differ from this version.

Although complete metabolism to an active drug, C2E2, was not observed in human skin in the current study, once in the systemic circulation, further hydrolysis of C2E5's metabolites can occur in the liver, mainly by CES1, and in plasma, possibly by paraoxonase and butrylcholinesterase as CES1 and 2 are not present (Bahar and Imai, 2013). Additionally, the metabolism of C2E5 by CESs in keratinocytes, which we report here, results in metabolites that are more hydrophilic than C2E5 and could potentially more readily enter the systemic circulation.

The differences in enzyme activity and expression among cell lines and skin tissue has important implications for future studies examining transdermal metabolism of ester-based prodrugs. HEKa, HEKn and HaCaT cell cultures have the potential for examining the metabolism of compounds that are substrates for CES2. However, of the human cell lines we examined, only HEKa cells have the potential for establishing the metabolism of compounds that are substrates for CES1.

In summary, this is the first study to characterize the expression of CES isoforms in multiple human skin cell lines and human skin tissue with a view to using native phase 1 enzymes in skin to enhance transdermal delivery of C2E5. The differences in enzyme activity and expression among cell lines and skin tissue has important implications for future studies examining transdermal metabolism of ester-based prodrugs. We confirmed that CES activity is present in skin, albeit at lower levels compared to the liver, and that CES2 activity, but not CES1 activity, in HEKa, HEKn and HaCaT cells is comparable to that of human skin. Consequently, human skin cell cultures may be useful in quantifying CES2-mediated drug metabolism. Of the human cell lines we examined, HEKa cells have the potential for establishing the metabolism of compounds that are substrates for CES1. However, precaution should be taken when human skin

cells lines are used as alternative models for human cutaneous metabolism in transdermal drug delivery. Since the CES1 specific inhibitor reduced human skin S9 fraction-mediated hydrolysis of C2E5, CES1 appears to be crucial for C2E5 metabolism; as a result, the HEKa cell line could be an appropriate model for metabolism of C2E5.

Acknowledgements

The authors wish to thank Dr. Zhi Liu's laboratory and Dr. Dhiren Thakker's laboratory for kindly providing experimental support.

Authorship Contributions

Participated in research design: Fu, Sadgrove, and Jay.

Conducted experiments: Fu

Performed data analysis: Fu, Sadgrove, Marson and Jay

Wrote or contributed to the writing of the manuscript: Fu, Sadgrove, Marson and Jay.

References

Bahar FG and Imai T (2013) Aspirin hydrolysis in human and experimental animal plasma and the effect of metal cations on hydrolase activities. *Drug Metab Dispos* **41:** 1450-1456.

Bencharit S, Morton CL, Howard-Williams EL, Danks MK, Potter PM, and Redinbo MR. (2002) Structural insights into CPT-11 activation by mammalian carboxylesterases. *Nat Struct Biol* **9:** 337-342.

Brzezinski MR, Abraham TL, Stone CL, Dean RA, and Bosron WF (1994) Purification and characterization of a human liver cocaine carboxylesterase that catalyzes the production of benzoylecgonine and the formation of cocaethylene from alcohol and cocaine. *Biochem Pharmacol* **48:** 1747-55.

Du L, Hoffman SM, and Keeney DS (2004) Epidermal CYP2 family cytochromes P450. *Toxicol Appl Pharmacol* **195:** 278-287.

Esser C and Gotz C (2013) Filling the gaps: need for research on cell-specific xenobiotic metabolism in the skin. *Arch Toxicol* **87:** 1873-1875.

Fu J, Pacyniak E, Leed MG, Sadgrove MP, Marson L, and Jay M (2015) Interspecies Differences in the Metabolism of a Multiester Prodrug by Carboxylesterases. *J Pharm Sci*. **105:** 989-995.

Fukami T, Takahashi S, Nakagawa N, Maruichi T, Nakajima M, and Yokoi T (2010) In vitro evaluation of inhibitory effects of antidiabetic and antihyperlipidemic drugs on human carboxylesterase activities. *Drug Metab Dispos* **38:** 2173-2178.

Hewitt NJ, Buhring KU, Dasenbrock J, Haunschild J, Ladstetter B, and Utesch D (2001) Studies comparing in vivo:in vitro metabolism of three pharmaceutical compounds in rat, dog, monkey, and human using cryopreserved hepatocytes, microsomes, and collagen gel immobilized hepatocyte cultures. *Drug Metab Dispos* **29:** 1042-1050.

Huckle JE, Sadgrove MP, Mumper RJ, and Jay M (2015a) Species-dependent chelation of (241)Am by DTPA Di-ethyl ester. *Health Phys* **108:** 443-450.

Huckle JE, Sadgrove MP, Pacyniak E, Leed MG, Weber WM, Doyle-Eisele M, Guilmette RA, Agha BJ, Susick RL, Mumper RJ, and Jay M (2015b) Orally administered DTPA di-ethyl ester for decorporation of (241)Am in dogs: Assessment of safety and efficacy in an inhalation-contamination model. *Int J Radiat Biol* **91:** 568-575.

Imai T, Takase Y, Iwase H, and Hashimoto M (2013) Involvement of Carboxylesterase in Hydrolysis of Propranolol Prodrug during Permeation across Rat Skin. *Pharmaceutics* **5:** 371-384.

Inoue M, Morikawa M, Tsuboi M, Ito Y, and Sugiura M (1980) Comparative study of human intestinal and hepatic esterases as related to enzymatic properties and hydrolizing activity for ester-type drugs. *Jpn J Pharmacol* **30:** 529-535.

Jewell C, Prusakiewicz JJ, Ackermann C, Payne NA, Fate G, and Williams FM (2007) The distribution of esterases in the skin of the minipig. *Toxicol Lett* **173:** 118-123.

Li P, Callery PS, Gan LS, and Balani SK (2007) Esterase inhibition by grapefruit juice flavonoids leading to a new drug interaction. *Drug Metab Dispos* **35:** 1203-1208.

Naik A, Kalia YN, and Guy RH (2000) Transdermal drug delivery: overcoming the skin's barrier function. *Pharm Sci Technolo Today* **3:** 318-326.

Nitti VW (2003) Transdermal therapy for overactive bladder: present and future. *Rev Urol* **5:** S31-6.

Perumal O, Murthy SN, and Kalia YN (2013) Turning theory into practice: the development of modern transdermal drug delivery systems and future trends. *Skin Pharmacol Physiol* **26:** 331-342.

Pindel EV, Kedishvili NY, Abraham TL, Brzezinski MR, Zhang J, Dean RA, and Bosron WF. (1997) Purification and cloning of a broad substrate specificity human liver carboxylesterase that catalyzes the hydrolysis of cocaine and heroin. *J Biol Chem* **272:** 14769-14775.

Prausnitz MR and Langer R (2008) Transdermal drug delivery. *Nat Biotechnol* **26:** 1261-1268.

Prusakiewicz JJ, Ackermann C, and Voorman R (2006) Comparison of skin esterase activities from different species. *Pharm Res* **23:** 1517-1524.

Saeki M, Saito Y, Nagano M, Teshima R, Ozawa S, and Sawada J (2002) mRNA expression of multiple cytochrome p450 isozymes in four types of cultured skin cells. *Int Arch Allergy Immunol* **127:** 333-336.

Satoh T, Taylor P, Bosron WF, Sanghani SP, Hosokawa M, and La Du BN (2002) Current progress on esterases: from molecular structure to function. *Drug Metab Dispos* **30:** 488-493.

Scheuplein RJ and Blank IH (1971) Permeability of the skin. *Physiol Rev* **51:** 702-747.

Sugibayashi K, Hayashi T, and Morimoto Y (1999) Simultaneous transport and metabolism of ethyl nicotinate in hairless rat skin after its topical application: the effect of enzyme distribution in skin. *J Control Release* **62:** 201-208.

Swanson HI (2004) Cytochrome P450 expression in human keratinocytes: an aryl hydrocarbon receptor perspective. *Chem Biol Interact* **149:** 69-79.

Tauber, U. R and Rost KL (1987) Esterase activity of the skin including species variations. *Pharmacology and the Skin* **1:**170-183.

Testa B and Mayer MJ (2006) The Hydrolysis of Carboxylic Acid Esters, in *Hydrolysis in drug and prodrug metabolism, chemistry, biochemistry, and enzymology* pp 365-418, Wiley-VCH publisher, Weinheim, Germany.

Thomsen R, Rasmussen HB, Linnet K, and INDICES Consortium (2014) In vitro drug metabolism by human carboxylesterase 1: focus on angiotensin-converting enzyme inhibitors. *Drug Metab Dispos* **42:** 126-133.

Wadkins RM, Hyatt JL, Wei X, Yoon KJ, Wierdl M, Edwards CC, Morton CL, Obenauer JC, Damodaran K, Beroza P, Danks MK, and Potter PM (2005) Identification and characterization of novel benzil (diphenylethane-1,2-dione) analogues as inhibitors of mammalian carboxylesterases. *J Med Chem* **48:** 2906-2915.

Wang JJ, Sung KC, Huang JF, Yeh CH, and Fang JY (2007) Ester prodrugs of morphine improve transdermal drug delivery: a mechanistic study. *J Pharm Pharmacol* **59:** 917-925.

Williams ET, Bacon JA, Bender DM, Lowinger JJ, Guo WK, Ehsani ME, Wang X, Wang H, Qian YW, Ruterbories KJ, Wrighton SA, and Perkins EJ (2011) Characterization of the expression and activity of carboxylesterases 1 and 2 from the beagle dog, cynomolgus monkey, and human. *Drug Metab Dispos* **39:** 2305-2313.

Williams FM (2008) Potential for metabolism locally in the skin of dermally absorbed compounds. *Hum Exp Toxicol* **27:** 277-280.

Zempsky WT (1998) Alternative routes of drug administration--advantages and disadvantages (subject review). *Pediatrics* **101:** 730-731.

Zhang Q, Grice JE, Wang G, and Roberts MS (2009) Cutaneous metabolism in transdermal drug delivery. *Curr Drug Metab* **10:** 227-235.

Zhang Y, Sadgrove MP, Mumper RJ, and Jay M (2013a) Radionuclide decorporation: matching the biokinetics of actinides by transdermal delivery of pro-chelators. *AAPS J* **15:** 1180-1188.

Zhang Y, Sadgrove MP, Sueda K, Yang YT, Pacyniak EK, Kagel JR, Braun BA, Zamboni WC, Mumper RJ, and Jay M (2013b) Nonaqueous gel for the transdermal delivery of a DTPA penta-ethyl ester prodrug. *AAPS J* **15:** 523-532.

Zhu QG, Hu JH, Liu JY, Lu SW, Liu YX, and Wang J (2007) Stereoselective characteristics and mechanisms of epidermal carboxylesterase metabolism observed in HaCaT keratinocytes. *Biol Pharm Bull* **30:** 532-536.

Legends for Figures

Figure 1. Structure of penta-ethyl ester DTPA prodrug (C2E5). ^{14}C-radiolabel positions are indicated by asterisks.

Figure 2. Log of relative expression of CES1 and CES2 mRNA in human epidermal keratinocyte HEKa, HEKn, HaCaT, A431 cells and human skin by RT-qPCR analysis. [A] CES1 expression. [B] CES2 expression. Values represent mean ± SEM (n=3).

Figure 3. Western blot analysis of human epidermal keratinocyte HEKn, HaCaT and A431 cells and human tissue. Each band was detected with CES1 and CES2 antibodies. [A] CES1 expression. [B] CES2 expression. Lane 1 = HEKn, 2 = HaCaT, 3 = A431, 4 = human skin, 5A = human liver, and 5B = human intestine.

Figure 4. Esterase and carboxylesterase activities in human epidermal keratinocyte HEKa, HEKn, HaCaT, A431 cells and human skin tissue measured with a *p*NPA and 4-NPV assay. [A] *p*NPA assay in the presence of S9 fractions of HEKa, HEKn, HaCaT, A431 cells and human skin. [B] 4-NPV assay in the presence of S9 fractions of HEKa, HEKn, HaCaT, A431 cells and human skin. The hydrolysis of the freshly prepared substrates was carried out in 96 well plates with a total volume of 100 µl/well. Reactions were initiated by mixing 1 µl of substrate with diluted S9 samples (0.1 mg/ml). The rates of hydrolysis of *p*NPA and 4-NPV were determined spectrophotometrically by measuring reaction products at 402 nm after 10 min incubation at 37°C using a UV spectrometer. Values represent mean ± SEM. (n=3).

Figure 5. C2E5 hydrolysis in human epidermal keratinocyte HEKa, HEKn, HaCaT, A431 cells. Loss of parent drug was measured by detecting changes in radioactivity of C2E5 at HPLC

elution peak (7.3 min) during a 60 min incubation of 1μM [^{14}C]-C2E5 with HEKa, HEKn, HaCaT and A431 cells. Values represent mean ± SEM (n=3).

Figure 6. C2E5 hydrolysis in human skin S9 fractions and inhibition studies on C2E5 hydrolysis. Inhibitors, benzil, trogliazone, loperamide, and BNPP were incubated with human skin S9 fractions for 30 min at 37°C before the reaction was initiated. Loss of parent drug was measured by detecting changes in spectromatogram at the LC/MS/MS analyte peak (3.6 min) after 120 min incubation of 0.5 μM C2E5 with human skin S9 fractions with and without inhibitors. Liver S9 fractions (1 mg/ml) were used as a positive control and boiled S9 fractions were used as negative controls. Values represent mean ± SEM (n=3).

DMD Fast Forward. Published on April 29, 2016 as DOI: 10.1124/dmd.116.069377
This article has not been copyedited and formatted. The final version may differ from this version.

Tables

Table 1. Esterase activity in human skin cell cultures, human skin S9 fractions and human liver S9 fractions

Cell Type	Hydrolytic activity (nmol/min/mg)
HEKa	20.2 ± 1.82
HEKn	31.6 ± 3.76
HaCaT	26.2 ± 1.97
A431	16.7 ± 1.11
Human skin	39.0 ± 11.54
Human Liver	167.2 ± 5.50

Data are the Mean ± SEM. N = 3.

Table 2. Carboxylesterase activity in human skin cell cultures, human skin S9 fractions and human liver S9 fractions

Cell Type	Hydrolytic activity (nmol/min/mg)
HEKa	40.9 ± 8.87
HEKn	125.8 ± 5.87
HaCaT	103.0 ± 9.65
A431	57.3 ± 7.56
Human skin	114.3 ± 5.60
Human Liver	217.7 ± 13.83

Data are the Mean ± SEM. N = 3.

Figure 1

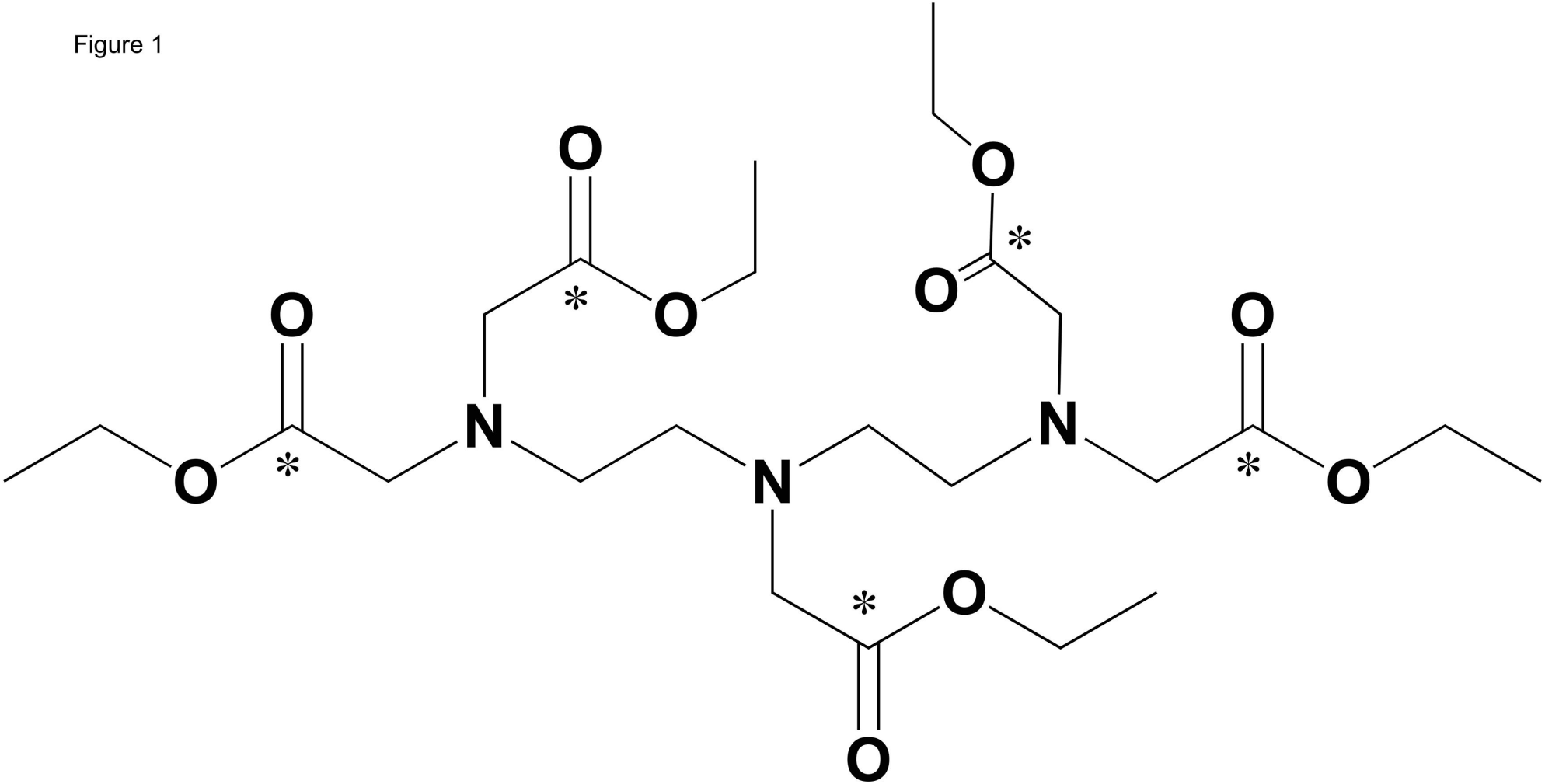

Figure 2

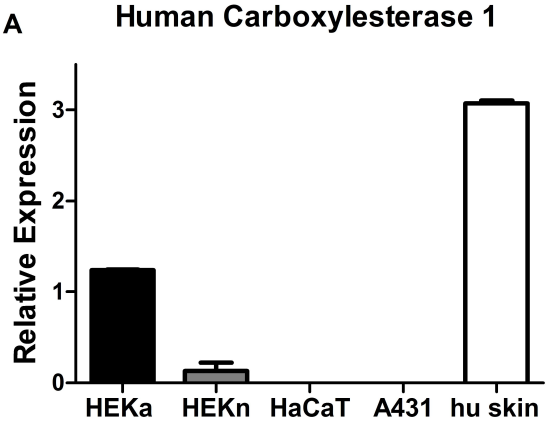
A
Human Carboxylesterase 1
Relative Expression
0
1
2
3
HEKa
HEKn
HaCaT
A431
hu skin

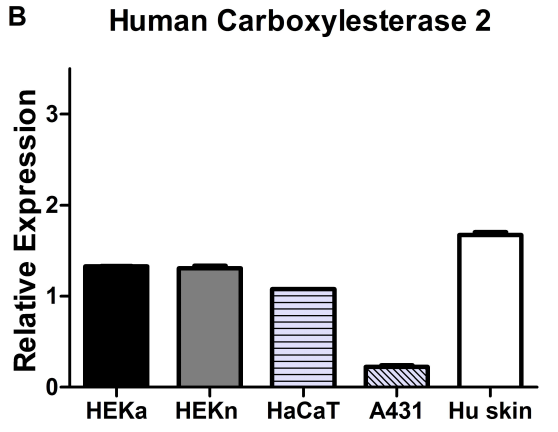
B
Human Carboxylesterase 2
Relative Expression
0
1
2
3
HEKa
HEKn
HaCaT
A431
Hu skin

Figure 3

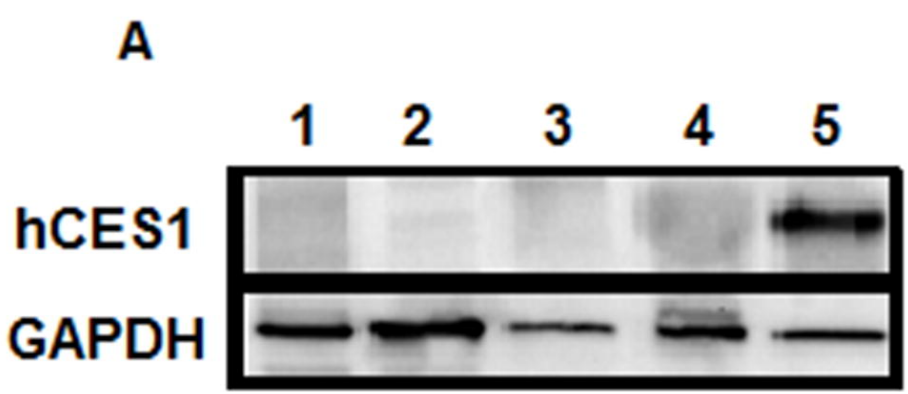

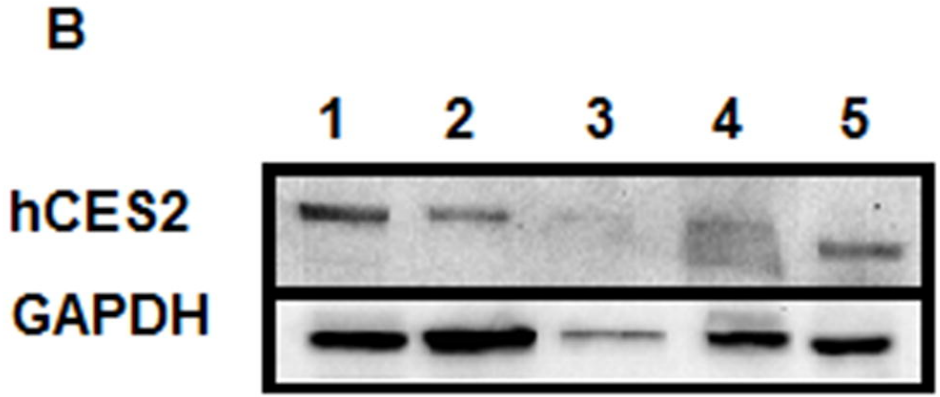

Figure 4.

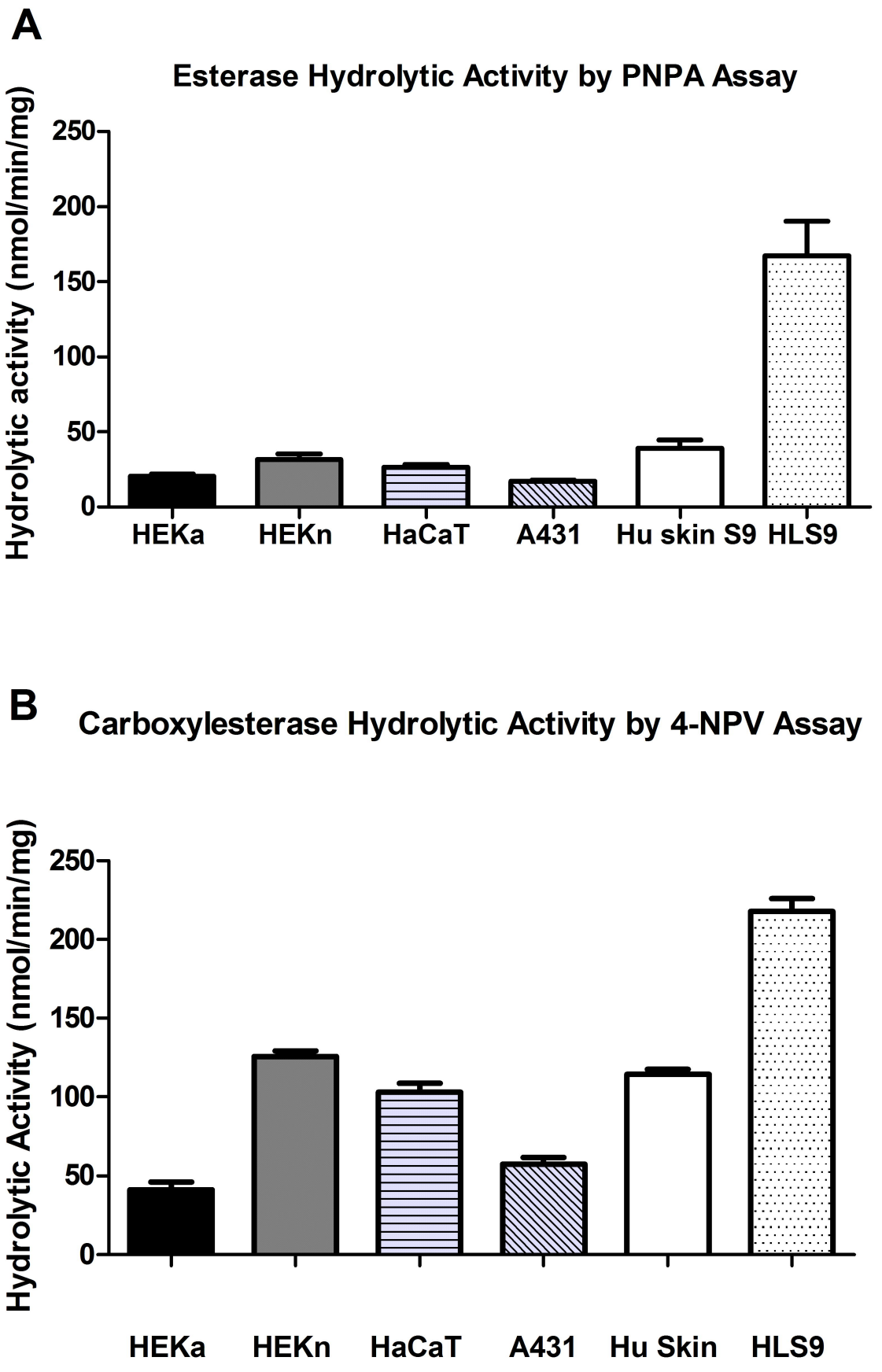
A
Esterase Hydrolytic Activity by PNPA Assay
Hydrolytic activity (nmol/min/mg)
250
200
150
100
50
0
HEKa
HEKn
HaCaT
A431
Hu skin S9
HLS9
B
Carboxylesterase Hydrolytic Activity by 4-NPV Assay
Hydrolytic Activity (nmol/min/mg)
250
200
150
100
50
0
HEKa
HEKn
HaCaT
A431
Hu Skin
HLS9

Figure 5

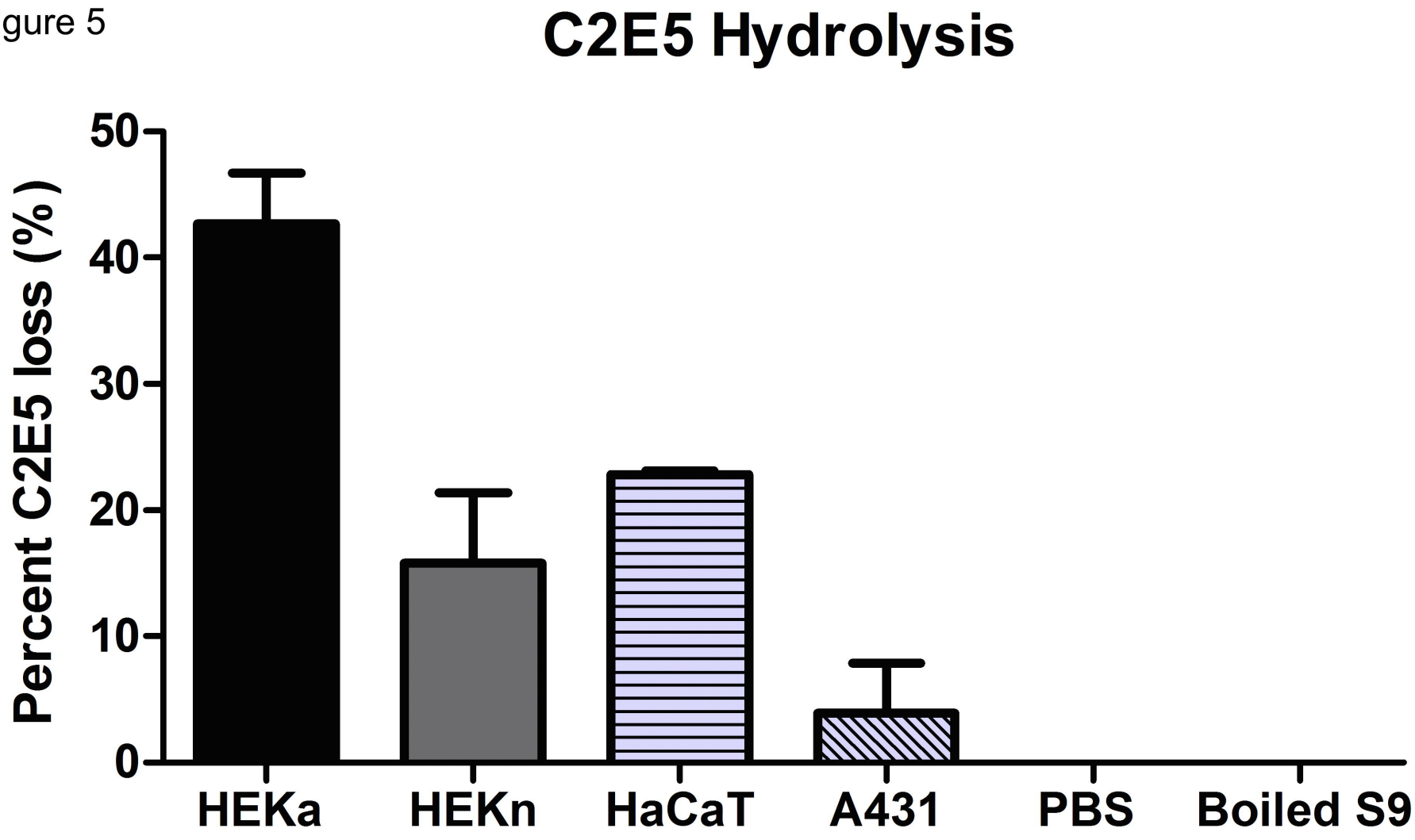
C2E5 Hydrolysis
Percent C2E5 loss (%)
50
40
30
20
10
0
HEKa
HEKn
HaCaT
A431
PBS
Boiled S9

Figure 6

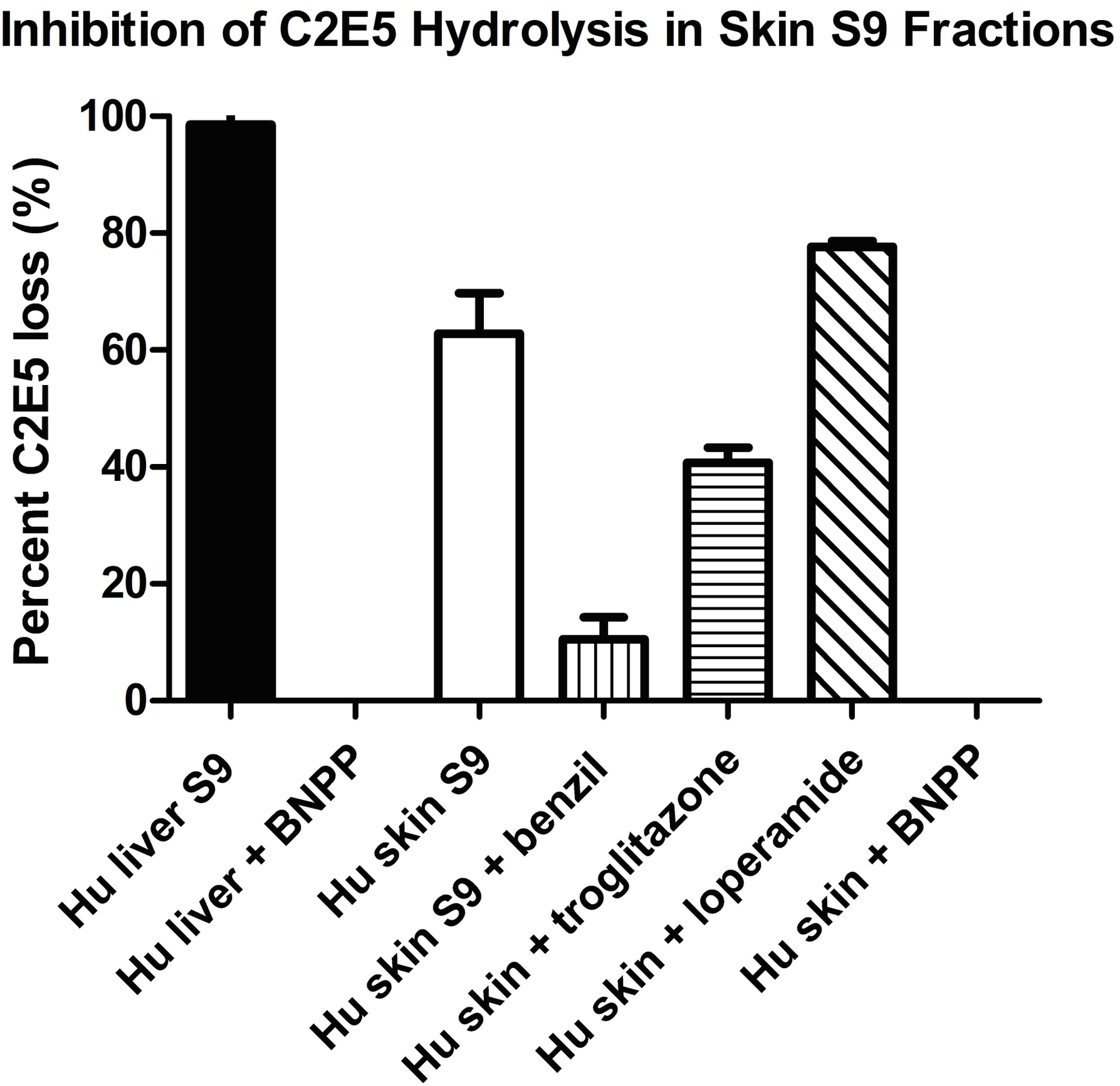
Inhibition of C2E5 Hydrolysis in Skin S9 Fractions
Percent C2E5 loss (%)
100
80
60
40
20
0
Hu liver S9
Hu liver + BNPP
Hu skin S9
Hu skin S9 + benzil
Hu skin + troglitazone
Hu skin + loperamide
Hu skin + BNPP